3D modeling of the stratigraphic and structural architecture of the Crotone basin (southern Italy) using machine learning with Python

Ettore Falsetta [a], Manuel Bullejos [b], Salvatore Critelli [a], Manuel Martín-Martín [c,*]

[a] *Dipartimento di Ingegneria dell'Ambiente, Università della Calabria, 87036 Arcavacata di Rende (CS), Italy*
[b] *Departamento de Álgebra, University of Granada, 18010, Granada, Spain*
[c] *Departamento de Ciencias de la Tierra y Medio Ambiente, University of Alicante, 03080 Alicante, Spain*

ARTICLE INFO

ABSTRACT

The 3D modeling and representation of geological data have experienced significant growth within last years, due to the use of new technologies derived from advancements in land representation methods. These technologies enable interactive, intuitive and clear geological visualizations. This paper shows how, by using the open-source Python software (operable with a simple internet browser) for machine learning (linear and KNN interpolations), together with Geographic Information Systems (GIS), it is possible to achieve interactive 3D visualizations of geological features in sedimentary basins. This study is performed in the onshore-offshore Crotone area (southern Italy) where a large amount of stratigraphic datasets are available from core perforation and seismic profiles due to the presence of a natural gas extraction field. Thanks to a database of 63 drilling lithologic records and 43 check points obtained from 9 interpreted seismic sections, several 3D HTML models were constructed defining three stratigraphic units (Pre-Messinian, Messinian, and Post-Messinian). An overlap of the Post-Messinian top surface and an erosional truncation of the Messinian top surface toward the N were observed, together with a rising of the Pre-Messinian top surface in the northwestern area. This stratigraphic architecture may indicate differential subsidence and/or uplifting due to syn-sedimentary fault kinematics in the whole studied area. The 3D models with the stratigraphic unit boundary surfaces obtained with KNN interpolation (showing stepped and abrupt edges) allowed the interpretation in terms of structural architecture and syn-sedimentary fault kinematics. Three main sets of faults were deduced: N–S; NNW-SSE, and ENE-WSW. A minorly represented E-W set was added to the main sets. These faults generated a horsts-grabens structure, and in many cases a determinate set of faults caused a progressive lowering or rising of some areas with an "en echelon" arrangement. According to previous works, these deduced sets of faults (most of them strike-slip faults) have a good agreement with the general structural architecture and defined faults in the area.

1. Introduction

In recent years, the traditional 2D visualization methods have been updated by three-dimensional (3D) models, providing an improvement in the visualization and analysis of geological features. In particular, the 3D geological modelling of the subsurface allows a comprehensive representation of the geological reality by integrating diverse data such as geological cross-sections and digital terrain models (DTM). These methodologies are increasingly successful due to their accessibility and ease of comprehension, compared to traditional visualization models. Moreover, the increase of subsurface data (seismic lines, boreholes, and other relevant data) and the development of efficient software and hardware further contribute to their popularity. Although various commercial software options for 3D geological analysis are widespread, many are costly and challenging to manage, while free alternative provide interesting results. The visualization of 3D geological elements by means of Python applications is successfully experimented in the interpolation of stratigraphic parameters derived from well drilling or classical geological information (Bullejos and Martín-Martín, 2023a, 2023b). This is testified by Bullejos et al. (2022a,b) and Martín-Martín et al. (2023a), who defined methodologies to create interactive 3D HTML models viewable through open-source applications. Accordingly, the Python applications are increasingly used in different geological fields with up-and-coming results in seismic (Bueno et al., 2020;
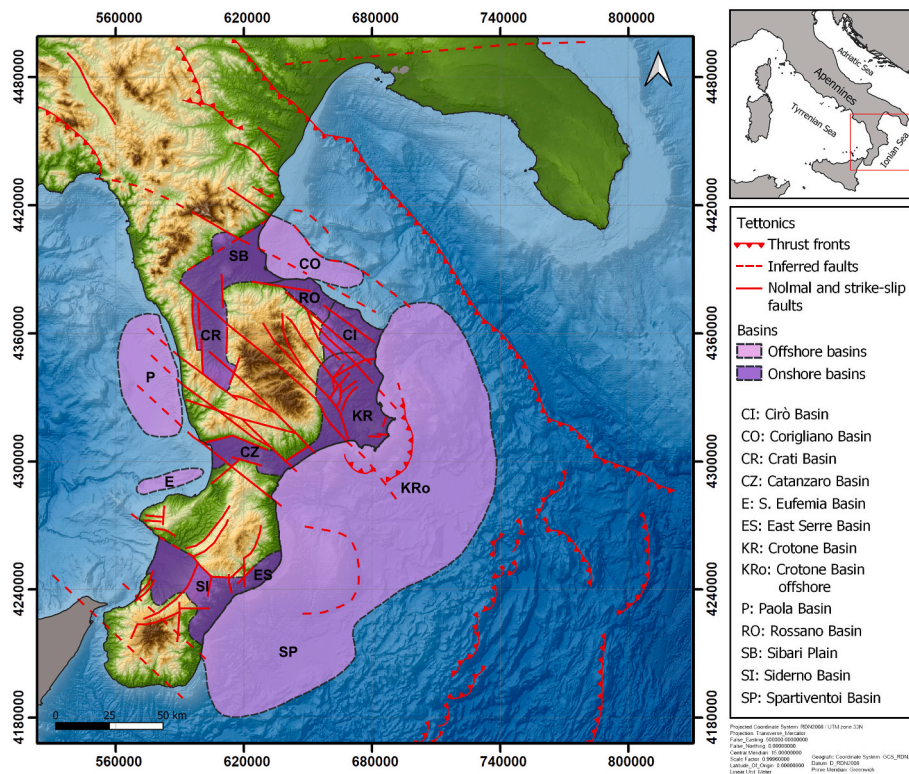

Fig. 1. Plio-Pleistocene basins formed by compressive tectonic activity (Modified from Zecchin et al., 2015).

Cavalcanti-Bezerra-Guedes et al., 2022), volcanic risk assessment (Tonini et al., 2015), well analysis (Fuentes et al., 2020), groundwater investigations (Matot et al., 2011; Memari and Clement, 2021), geophysical exploration (Krieger and Peacock, 2014), paleontological (Casanova-Arenillas et al., 2020), and mineralogical studies (Scharf et al., 2022), geomorphological, and engineering projects (Adamczyk and Tiede, 2017; Rivillas-Ospina et al., 2022). The main focus of these kind of researches points to the automation and the statistical analysis of big datasets from different sources, including the monitoring of physical properties (Matot et al., 2011; Adamczyk and Tiede, 2017; Memari and Clement, 2021; Rivillas-Ospina et al., 2022), seismic profiles (Krieger and Peacock, 2014; Tonini et al., 2015; Bueno et al., 2020; Cavalcanti-Bezerra-Guedes et al., 2022), and drilling data (Fuentes et al., 2020; Casanova-Arenillas et al., 2020). In this article, multiple HTML files were generated from boreholes and seismic profiles by means of Python applications, that return, as an output, a series of interactive multi-perspective 3D models. The project was experimented in the Crotone Basin (southern Italy) because of the wide spectrum of data availability and the peculiar geological characteristics of the investigated area. These HTML models allowed visualizing the stratigraphic architecture of the Neogene sedimentary infill and the structural partition of the Crotone Basin, simply using a standard web browser. Understanding the complex subsurface geological structures is essential for any land planning and design strategy in the perspective of integrated environmental technologies. Therefore, constructing 3D geological models is fundamental for both scientific and applied research in the earth sciences field, as well as for environmental protection, geological risk assessment, and territorial planning.

2. Geological setting

The Crotone Basin is one of the most extensively studied Neogene basins in Italy (Van Dijk, 1991, 1994; Van Dijk and Okkes, 1991; Van Dijk et al., 2000; Zecchin et al., 2013a, 2013b, 2015, 2018, 2020; Conforti et al., 2014; Brutto et al., 2016; Tripodi et al., 2013, 2018;

Critelli, 2018; Critelli and Martín-Martín, 2022, 2024; Mangano et al., 2023a, 2023b; Martín-Martín et al., 2023b), located between the eastern margin of the Sila Massif and the Ionian Sea. It consists of a depocenter filled with sediments ranging from deep marine to continental setting, with ages spanning from the Serravallian to the Pleistocene. These sediments are organized into major and minor tectono-sedimentary cycles (Roda, 1964; Van Dijk, 1990, 1991; Massari et al., 2002; Zecchin et al., 2003a,b; 2004a, Zecchin, 2005, 2015; Mellere et al., 2005). The Crotone Basin is bounded to the northeast and southwest by two main left-lateral strike-slip fault zones NW-SE oriented (the Rossano-San Nicola, to the north, and the Petilia-Sosti, to the south) but other sets of faults E-W (as the Strongoli fault), N–S (as the Melissa fault) and WSE-ENE (as the Isola di Capo Rizzuto fault) and SW-NE (as the Rocca di Neto fault) oriented are also present (Zecchin et al., 2012, 2013a, 2013b, 2020). Its development has been associated with the southeastward migration of the Calabrian terranes (Critelli, 1993, 1999, 2018; Bonardi et al., 2001; Zecchin et al., 2004a, 2011, 2013a, 2013b, 2020; Barbera et al., 2011; Perri et al., 2012; Brutto et al., 2016; Tripodi et al., 2013, 2018; Corrado et al., 2019; Campilongo et al., 2022; Criniti et al., 2023a, b; Costamagna and Criniti, 2024), resulting in the subduction of the Ionian crust and the opening of the Tyrrhenian Basin, starting from the Serravallian/Tortonian (Patacca et al., 1990; Van Dijk, 1990, 1991; Van Dijk and Okkes, 1990, 1991; Knott and Turco, 1991; Van Dijk and Scheepers, 1995; Le Pera and Critelli, 1997; Mattei et al., 2002; Critelli, 2018; Critelli and Martín-Martín, 2022, 2024; Criniti et al., 2023a).

2.1. Main tectonic episodes

The depositional history of the Crotone Basin has been primarily accompanied by a local extensional regime, linked to the extension of the forearc region, as evidenced by normal synsedimentary faults during the Plio-Pleistocene which also controlled the basins development (Moretti, 1993; Massari et al., 2002; Zecchin et al., 2003a,b; 2004a, 2020). However, this extensional regime has been episodically interrupted by deformative events with a compressional component, possibly
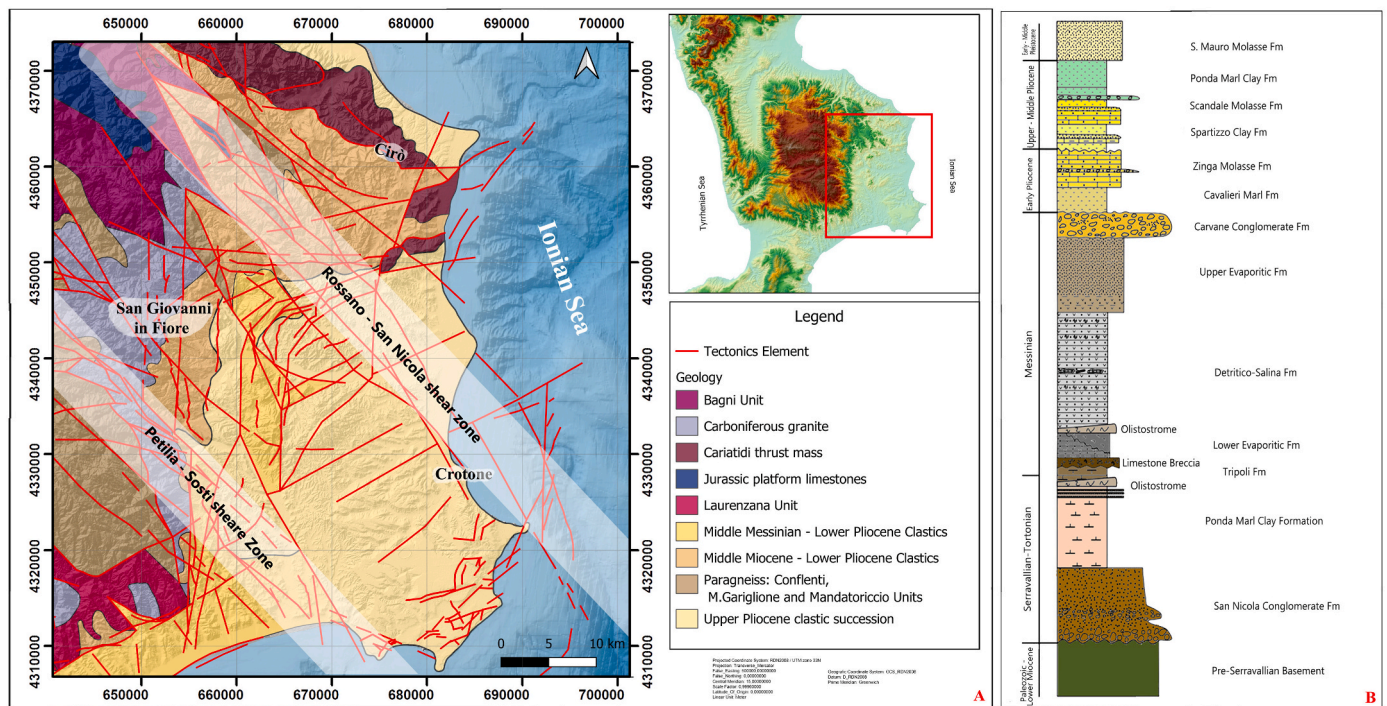
Fig. 2. A) Fault sets of the Crotone Basin (Modified after Van Dijk and Okkes, 1990; Van Dijk et al., 2000); B). Stratigraphic section of the Crotone Basin (Modified from Roda (1964), Critelli (1999), Barone et al. (2008) e Critelli et al. (2011, 2014a, 2014b).

related to the transpressive activation of the NW-SE strike-slip zones during the Messinian, the Zanclean and Piacenzian, and the middle Pleistocene (Roda, 1964; Van Dijk, 1990, 1991; Van Dijk and Okkes, 1990, 1991; Van Dijk et al., 2000; Massari et al., 2002; Zecchin et al., 2004; Muto et al., 2014, 2017). These movements led to the formation of diverse Plio-Pleistocene basins (Fig. 1) during and after the main phases of compressive tectonic activity (Zecchin et al., 2015).

Minor tectonic events are also recorded within the succession. In fact, several basin-scale tectonic events were also evidenced (Zecchin et al., 2020; Arcuri et al., 2023): (1) the extensional Serravallian-Tortonian event coeval with the opening of the southern Tyrrhenian Sea and peri-Tyrrhenian basins and with the opening of the Crotone Basin; (2) the Messinian compressive or transpressive event responsible of the uplift for the Cirò area and the formation of a E-W elongated foredeep in the northern part of the Crotone area; (3) the extensional or transtensive Pliocene event causing halokinesis dome structures of Messinian evaporaites due to normal faulting; and (4) the contractional or transpressional Pleistocene event associated with the end of the migration of the Calabrian terranes toward the Apulian plate. These deformative phases resulted in widespread uplift and the formation of unconformities (Roda, 1964; Van Dijk, 1990; Zecchin et al., 2003a,b; 2004a). Throughout Northern Calabria and particularly in the Crotone Basin, numerous sets of faults (Fig. 2A) are recognized on a regional scale, which can be grouped into three main patterns (Van Dijk and Okkes, 1990, 1991): (1) the first pattern includes a set of faults related to extensive strike-slip zones NW-SE oriented; (2) the second pattern includes a set of faults related to extensive strike-slip zones SW-NE oriented; and (3) the third pattern includes all recent sets of faults associated with the uplift of the onshore area. For the onshore area, the activity of these sets of faults is dated to late Miocene-middle Pliocene. The deposits exhibit clear synsedimentary features, and numerous indications highlight the role of these faults in generating various unconformities that separate sedimentary sequences. The set of faults associated with the third pattern can be linked to the uplift of the Sila Massif, which began in the Pleistocene. This pattern includes set of faults with NE-SW, NNE-SSW, and NNW-SSE orientations, affecting

rocks from the Messinian to the Recent.

Since the middle Pleistocene, after the deposition of sandy-silt deposits transitioning rapidly to reddish beach sands ("San Mauro Formation"; Roda, 1964; Di Grande, 1967), the Calabrian terranes underwent significant uplift, leading to the emergence of various basins, including large portions of the Crotone Basin.

2.2. Lithostratigraphy of the Crotone basin

Since the 1960s, numerous studies have focused on the stratigraphy of the Crotone Basin. Based on previous works (Roda, 1964 Critelli, 1993, 1999, 2018; Barone et al., 2008; Critelli et al., 2011, 2014a,b, 2017; Arcuri et al., 2023), the stratigraphic succession of the Crotone Basin, as exposed, can be summarized as follows (Fig. 2B). The stratigraphic succession of the Crotone Basin unconformably overlies the crystalline basement with a Pre-Evaporitic Unit formed of about 200 m in thickness of alluvial conglomerates and breccias of the San Nicola dell'Alto Formation (Ogniben, 1955) (Serravallian-Tortonian). At the top of this unit lies a marine succession of pelitic-marly and pelitic-sandy deposits referred to as the Ponda Marl Clay Formation (Ogniben, 1955; Roda, 1964) (Tortonian-Messinian), with an outcrop thickness of about 200 m, but in some wells, it can reach values exceeding 1 km. In the upper part of the Ponda Marl Clay Formation, lies an Olistostrome of Variegated Clays, approximately 200 m thick, characterized by a variegated and varicolored clay matrix containing blocks of pelagic limestones, sandstones, and more or less silicified argillites. Above it, the clay-marly-diatomaceous formation of the Tripoli Formation (Messinian), that is an excellent stratigraphic marker, occur with a thickness of few tens of meters. Above the Tripoli Formation, there is the Messinian succession, consisting of two main units: the "Calcareous-Evaporitic" Unit and the "Lago-Mare" Unit. The "Calcareous-Evaporitic" Unit is represented by the Gypsum Formation (Critelli et al., 2014a,b) of over 400 m thick, including gypsum clastic facies, from dominant gypsum sandstones to gypsum breccias, nodular gypsum, and halite. An extensive erosional surface resulting from a new sea level dropping, separates the "Calcareous-Evaporitic" Unit from the subsequent "Lago-Mare" Unit
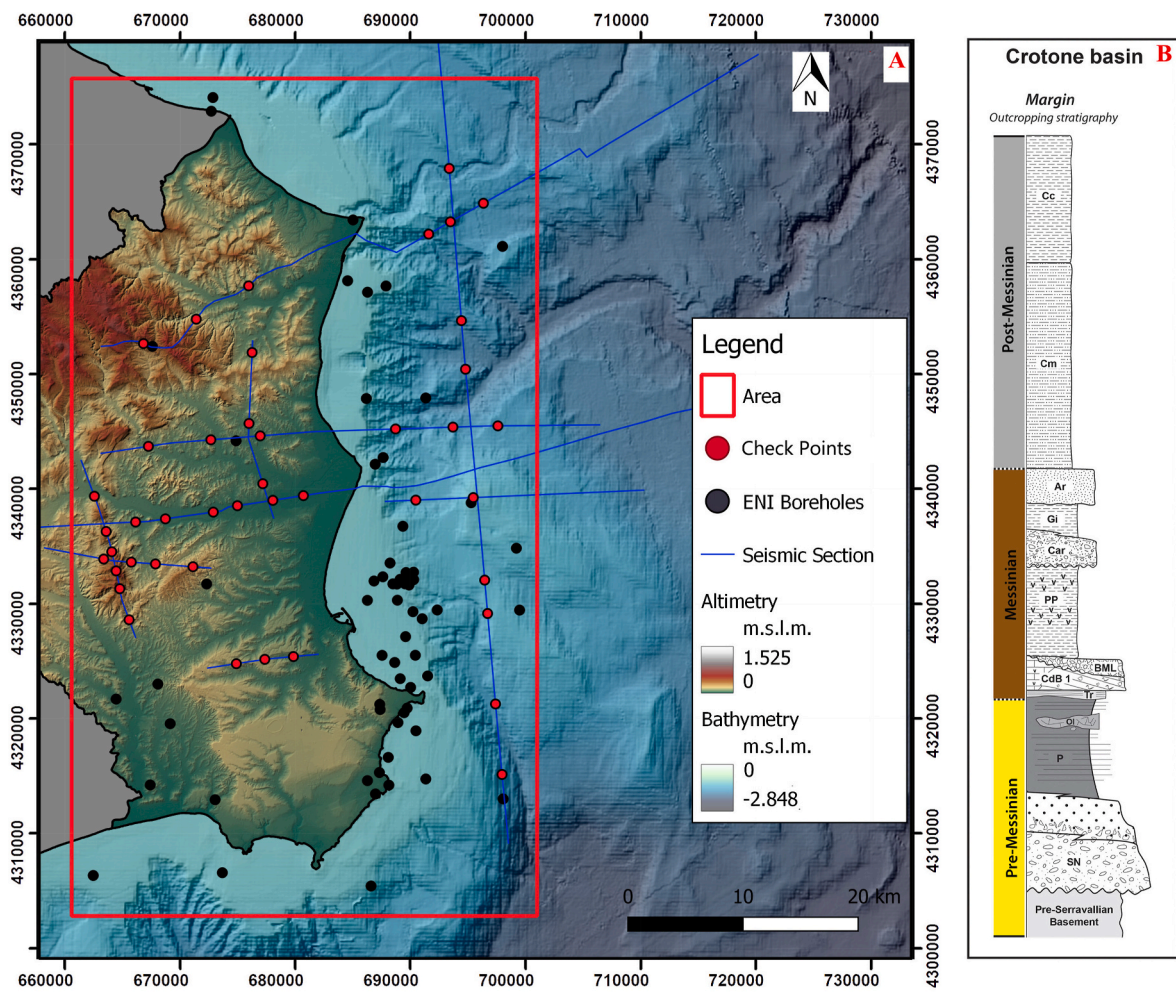
Fig. 3. A) Simplified sketch map of the Crotone area showing the ENI boreholes data and check points deduced from seismic profiles (red points) data; B) Stratigraphic architecture of the Crotone Basin (Modified from Borrelli et al., 2022).

(total thickness of about 250 m), characterized, from bottom to top, by alluvial conglomerate of the Carvane Formation. The stratigraphic sequence continues with the Plio-Pleistocene succession, characterized at the base by the Cavalieri Marls Formation (maximum thickness of about 200 m), passing upward to the sandy deposits of the Zinga Molasse Formation (Roda, 1964). Successively, there are the Plio-Pleistocene arenitic-pelitic formations of the Spartizzo Clays and the Scandale Molasse formations (maximum thickness of about 200 m both). The entire sequence is then covered by the Cutro Clays Formation (Piacenzian-middle Pleistocene), with an outcrop thickness of about 350 m reaching up 1200 m in the subsurface, representing a marine environment. The stratigraphic succession terms with the Pleistocene San Mauro Formation (approximately 200 m thick), consisting of predominantly arenitic deposits representing the infilling of submarine canyons formed due to the generalized uplift of the Crotone Basin. In the offshore area, the Plio-Pleistocene stratigraphic sequence reaches thicknesses of up to 2400 m and is characterized by clayey deposits representing deep basin environments referred to as the Crotone Clays Formation (ENI nomenclature). Several first-order strata surfaces at the lower Serravallian (basal unconformity), upper Messinian, and mid-Pliocene; as well as, second-order ones at the Tortonian, intra-Messinian, Zanclean, lower Pleistocene, mid-Pleistocene were proposed (Zecchin et al., 2015, 2020) separating first-order (Serravallian-Messinian, uppermost Messinian-Zanclean, and Piacenzian-upper Pleistocene) and second-order (Serravallian-lower Tortonian, Tortonian, lower Messinian, upper Messinian, uppermost Messinian-lower Zanclean, upper Zanclean, uppermost Zanclean, Piacenzian-lower Gelasian, upper Gelasian-Calabrian, and uppermost Calabrian-upper Pleistocene) stratigraphic sequences.

3. Methodology

The lithological dataset was built starting from ENI databases, made up in collaboration with University of Calabria during the project named "Definition of the Geological Model and Geodynamic Phenomena of the Crotone Basin". The dataset comprises 63 lithological records obtained from drilling exploration located in the study area, including 1 onshore and 47 offshore boreholes (Fig. 3). The areas with scarce or without information of direct boreholes, were implemented with 43 check points obtained from the 9 interpreted seismic sections existing in the area (Criniti et al., 2023a; Mangano et al., 2022, 2023a, 2023b). A dataset of 106 boreholes-check points, representing the whole studied area, are explained in Fig. 3A. All the data were carefully reviewed and reprocessed with the aim of ensuring that the dataset is free from any anomalies and characterized by a homogeneous set of data suitable for the intended purpose. In this paper, the deposits belonging to Crotone Basin have been renamed and divided into three main units (Fig. 3B). Pre-Messinian unit includes all the deposits layer before the Messinian salinity crisis event, that passes upward to a Messinian unit, which comprises deposits accumulated during the Messinian period. Post-Messinian unit (or Plio-Quaternary unit), that encompasses deposits formed after the Messinian salinity crisis event. The division into these three main units was performed in order to simplify and group the deposits and facilitate the analysis and interpretation of the analyzed geological data. It is essential to emphasize that this division was adopted for demonstrative purposes and should not be interpreted as a complete and detailed representation of the complex stratigraphy of the Crotone Basin. Another classification may have been made if the purposes were others.

As shown in Fig. 3B, the stratigraphic architecture of the Crotone Basin is much more complex and articulated. Each stratigraphic unit comprises multiple formations with lateral passages and/or deletions and overlaps due to erosion, that make up the basin. The Pre-Messinian deposits are characterized by a transgressive pre-evaporitic unit of Serravallian-Tortonian age, overlying a crystalline basement. This unit is characterized by Serravallian conglomerates and sandstones belonging to the San Nicola Fm (SN), that passes upwards into the Tortonian grey clays of the Ponda Fm (P). The latter is followed by the diatoms of the Tripoli Fm (Tr), indicating the maximum depth of the depositional system (Zecchin et al., 2013a, 2013b; Borrelli et al., 2022). The Messinian deposits are characterized by two major units, defined by Gindre-Chanu et al., 2020, as "Calcareous-Evaporitic" Unit and "Lago-Mare" Unit. The "Calcareous-Evaporitic" Unit begins with the Calcare di Base Fm (CdB) that indicates the presence of a carbonate-evaporite platform-to-slope system (Gindre-Chanu et al., 2020; Borrelli et al., 2021, 2022). Above it, there is a clastic body characterized by very coarse disorganized breccias and debrites comprising gypsum, carbonates, and terrigenous clasts (Borrelli et al., 2022), part of what is known as Breccia di Madama Lucrezia (BML). This first unit ends with clays and clayey marls covered by sulfates and clay deposits (Petilia Policastro Fm – PP). The "Lago-Mare" Unit follows upward with a thick conglomerate body (Carvane Conglomerate Fm – Car), covered by clays (Gigli Fm – Gi) and sandstones (Arvano Fm – Ar) (Massari et al., 2010; Massari and Prosser, 2013; Borrelli et al., 2022). Finally, the Post-Messinian deposits (or plio-quaternary deposits) are characterized by clay deposits of Plio-Pleistocene age, including the Cavalieri Marl Fm and the Cutro Clay Fm (Perri et al., 2024). The data of the defined stratigraphic units (Pre-Messinian, Messinian and Post-Messinian) have been compiled into an XLS (Excel) file containing the boreholes locations and their position on seismic profiles in the form of UTM coordinates and the elevation values of the top and bottom of the three defined classes during the data homogenization phase. The elevation (Z) is measured in meters, and the boreholes coordinates (X and Y) are organized to define a georeferenced matrix of geological data projected in space and depth. Once the data are in the XLS file the python processing can be made. The methodology similar to that given in Bullejos et al. (2022a,b, 2023), Bullejos and Martín-Martín (2023a,b), Martín-Martín et al. (2023a) to process the data, was used. In particular Pandas package was adopted for data analyses and manipulation with a consequent transformation of the original XLS files with the borehole or seismic data are transformed into Pandas data frames. The Numpy scientific package was then used for scientific computing, Numpy allowed to create and manipulate lists which are the basic data for plotting. The interpolation process interested the Python Numpy extension Scipy, whereas for the plotting of the data and for obtaining of the output files with the models, the graphical libraries Plotlib and Matplotlib were used. We also defined custom functions to do mathematic computations and to automatize plotting processes. The coast line in the models is obtained by means of a track traced with Google earth. This track was treated to obtain the UTM coordinates and the elevation of the points in it. We also used Python for this work and in particular the Copernico Python package. Numpy and Copernico were also employed to define a grid that cover the study area, with a successive linear interpolation to obtain a real topography of the area. In the data the lists of points that mark the beginning and end of each defined stratigraphic units in each borehole or check-point, is present. Two types of interpolation on these points were used, to define the surfaces that limit the different defined stratigraphic units. A linear interpolation makes smoother the transition between points for stratigraphic interpretations, and a KNN interpolation modeled sharper surfaces that give us clues to deduce the structural architecture of the basin.

Thus, both interpolations give relevant geological information on the basin. Also, horizontal x-spaced and serial vertical cross-sections have been performed again using machine learning K-nearest neighbors algorithm and in particular we used the Python package sklearn.neighbor. To use the KNN algorithm we have to fill the gaps in our data by adding data in each borehole every meter this makes our data lists much larger and unwieldy but python can handle huge amount of data despite which increases the computation time. When we used the KNN algorithm we have to choose the parameters K and weights. When K = 1 is chosen, as we have done, to predict the value of a new point, the algorithm will search for the closest point in the data. On the other hand, the weights parameter could be 'uniform' or 'distance'. We have chosen 'distance' to weight the decision. Finally, the solid bodies (volumes) have been also calculated using Convex Hulls. The Convex Hull of a set of points X in space is the smallest convex polyhedron in three dimensions that encloses all points in X the methodology used is similar to that we explain in Bullejos et al. (2022a,b, 2023) and Martín-Martín et al. (2023a). With this methodology the next 2D or 3D HTML models have been constructed: (1) topographic surface and boreholes location including check-points from seismic profiles (Fig. 4); (2) horizontal 100 m-spaced geological sections (Fig. 5); serial vertical geological cross-sections (Fig. 6); boundary surfaces among the stratigraphic defined units with linear interpolation (Fig. 7); boundary surfaces among the stratigraphic defined units with KNN interpolation (Fig. 8); Convex Hull volumes of the stratigraphic defined units (Fig. 9). This information has been later analyzed using stratigraphic and structural universal criteria in order to obtain details on the stratigraphic and structural architecture of the Crotone Basin. So, vertical sections (Fig. 4) and boundary surfaces with linear interpolation (Fig. 7) have been reinterpreted in term of stratigraphic architecture and subsiding areas in Fig. 10. Moreover, vertical sections (Fig. 4) and boundary surfaces with KNN interpolation (Fig. 8) have been reinterpreted in term of structural architecture and fault actuation in the basin in Figs. 11 and 12.

4. Results

The dataset has been divided and arranged into three main stratigraphic units: pre-Messinian, Messinian, and post-Messinian (or Plio-Quaternary). By using two different interpolation methods (linear and KNN) and the Convex Hull construction we have obtained 2D and 3D models with the stratigraphic defined units consisting in: boreholes net and topographic surface, serial horizontal sections, serial vertical sections, stratigraphic surfaces separating the stratigraphic defined units, and volumes of the stratigraphic defined units.

4.1. Boreholes net and topographic surface

The boreholes and check-points from seismic profiles information allowed to construct a 3D HTML model where stratigraphic units were represented in the columns with different colors (Pre-Messinian in yellow, Messinian in orange, Post-Messinian in grey). From this 3D HTML model, Fig. 4 details the topographic and sea-level surface, the boreholes and the stratigraphic units from each borehole. In each borehole the thickness of each stratigraphic unit can been estimated.

4.2. Serial 100 m-spaced horizontal sections

Also, a 3D HTML model with a serial 100 m-spaced of horizontal sections representing the three stratigraphic units is presented. According to this model, Fig. 5 was constructed using only 500 m-spaced horizontal sections. Examples of Intermediate zenithal-lateral views at 0, - 500 m, - 1000 m, - 1500 m, - 2000 m, and - 3000 m are shown. Fig. 5 shows the progressive reduction up to the complete absence of the Post-Messinian unit and its replacement by the Messinian and Pre-Messinian units. Moreover, Messinian unit is always restricted to the S and central area.

4.3. Serial vertical sections

Five 2D vertical sections were created in order to cover the study area with the boreholes and the check points from seismic profiles. These sections were then exported to png files representing the three stratigraphic units with a vertical representation from 3.000 m below sea level (b.s.l.) to 500 m above sea level (a.s.l.). The transversal sections A, B and C(from south to north) were oriented W-E while the longitudinal ones (D and E, from west to east) were oriented S–N. Horizontal scales (X–Y) are the same for constructing the 5 sections but vertical scale (Z) is enhanced in order to better see the thin Messinian intermediate unit. With these vertical cross-sections, Fig. 6 was composed. Sections show an overlap of the Post-Messinian unit and an erosional truncation of the Messinian unit toward the N. Also, a rising of the Pre-Messinian unit in the north area is visible (left part of section C). Sections also show important changes in thickness of all stratigraphic units, despite no information can be provided about the thicknesses of the lower stratigraphic unit since it has been affected by erosion after their deposition and because the depth of investigation was limited to 3.000 m b.s.l. In the case of the Messinian unit changes in thickness are evident from one sector to others from about 2.000 m of maximum thickness in the left part of sections B and E to about 200 m thick in left parts of
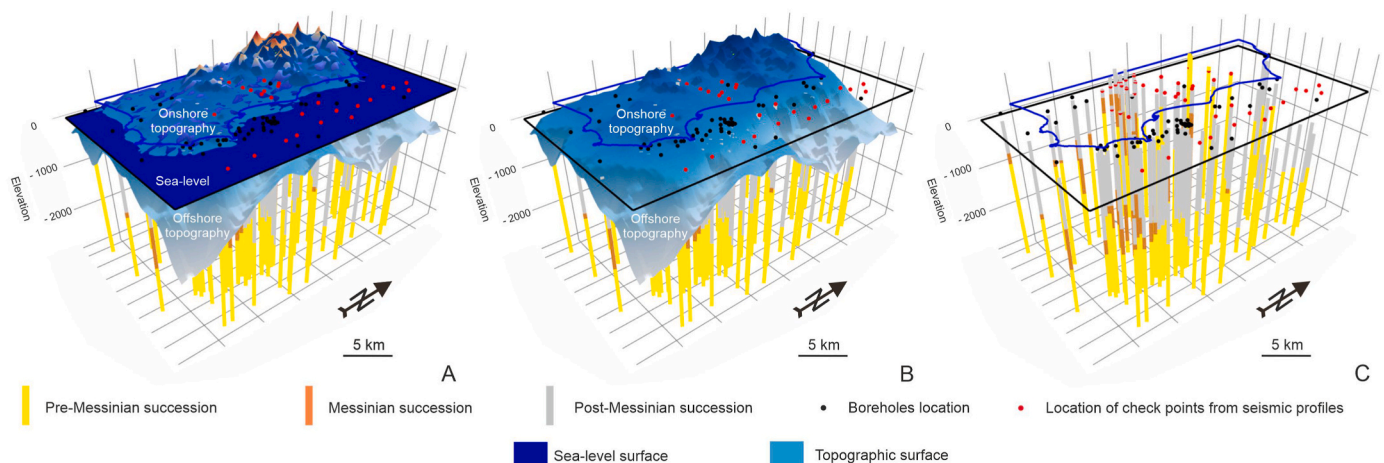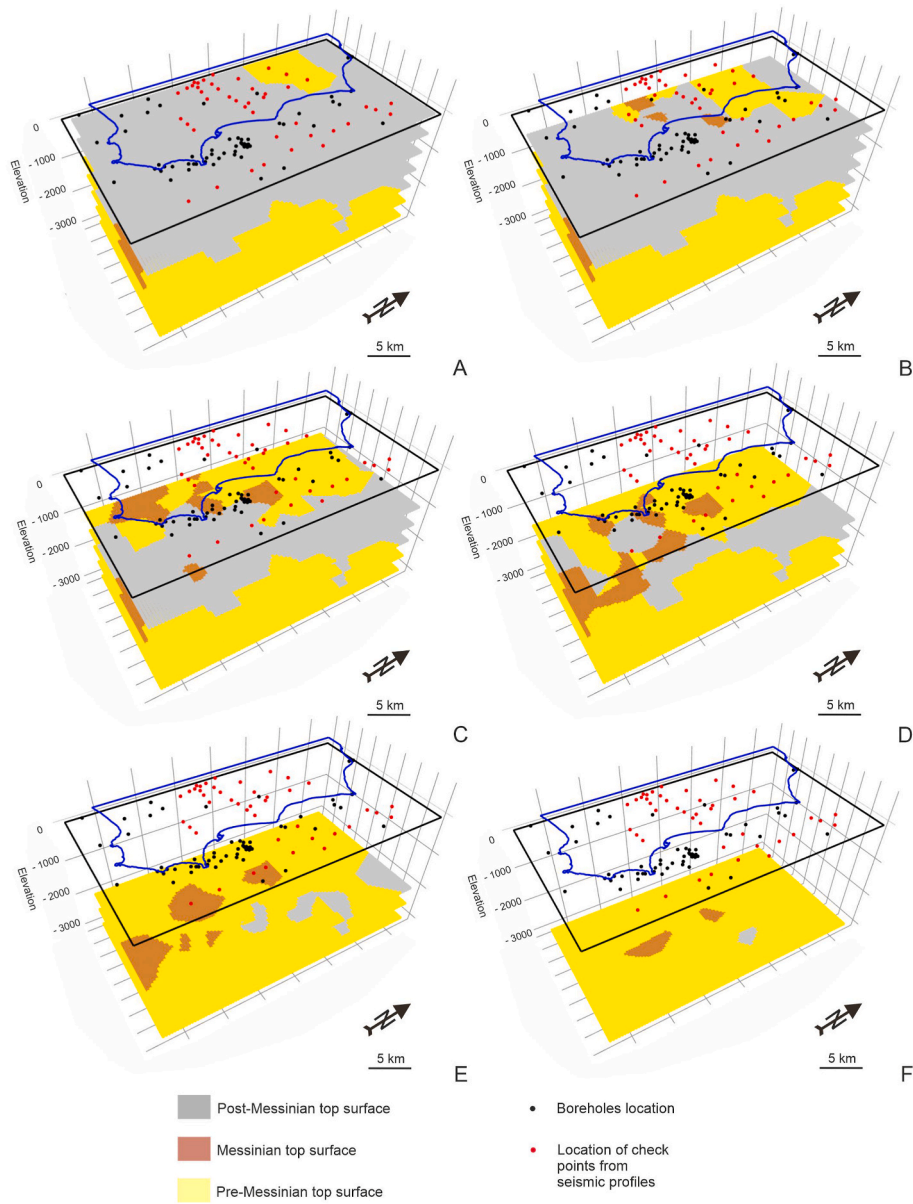

Fig. 4. Intermediate zenithal-lateral views of the 3D HTML model with the boreholes net (black points) and the check points from seismic profiles (red points) with the defined stratigraphic units and topographic and sea-level surfaces: A) view of the full 3D representation with topographic surface and sea-level surface: B) view of the 3D representation with topographic surface and the boreholes-check points net; C) view of the 3D representation only with the boreholes-check points net.

Fig. 5. Intermediate zenithal-lateral views of the 3D HTML model with 100 m-spaced horizontal sections obtained with KNN interpolation: A) example at 0 m depth; B) example at - 500 m; C) example at – 1000 m; D) example at - 1500 m; E) example at – 2000 m; F) example at – 3000 m.
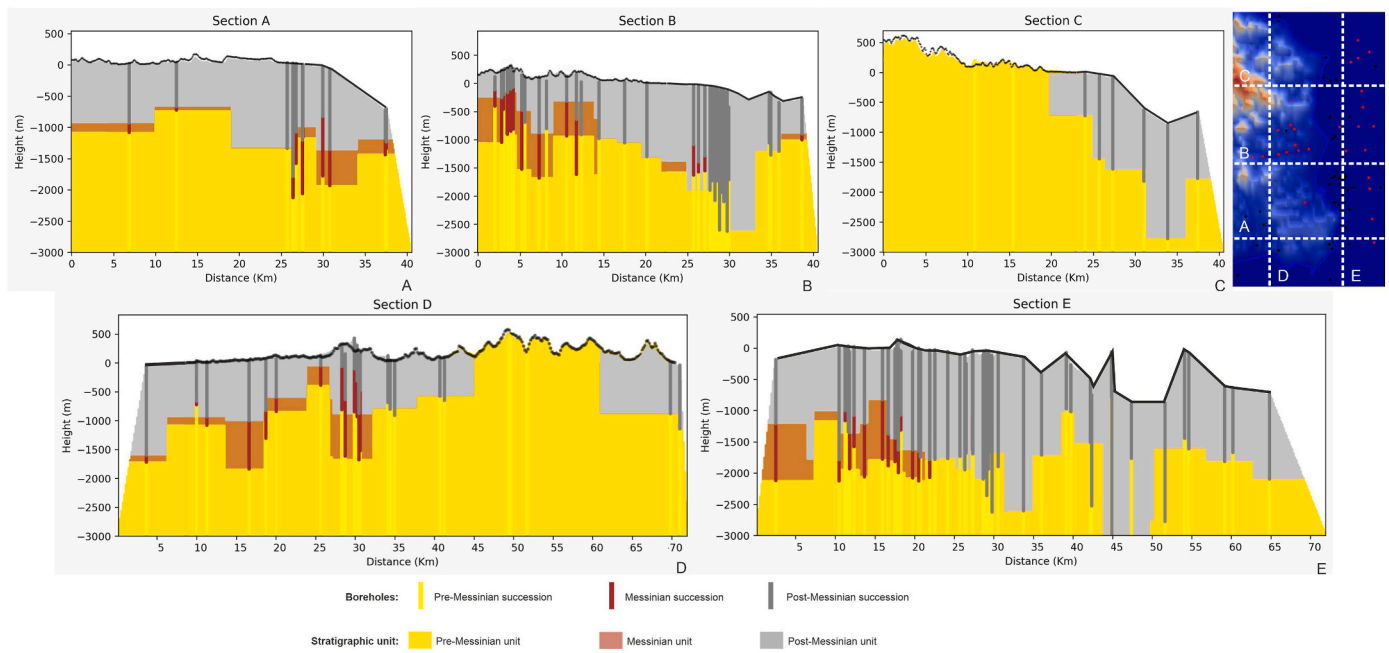
Fig. 6. Vertical sections obtained with KNN interpolation and exported as png files with sketch index map in the right-up corner. A to E) sections A to E.

section A and D, and right part of section B. A progressive reduction in the thickness of the Messinian unit is also testified toward the north and east in sections B and E. This stratigraphic unit is completely missing in Section C but also in the west part of sections D and E after a progressive reduction in thickness (corresponding in all these cases with the northern part of the study area). The upper stratigraphic unit is always recorder in all sections but it is limited in the left part of section C and the middle-right one in section D. The thickness from this unit reaches more than 2.500 m in the right part of sections B and C and in the middle-right part of section E. In other cases, a very constant thickness of about 1.000 m is evidenced.

4.4. Stratigraphic surfaces obtained with linear interpolation

A new 3D HTML model was performed by using linear interpolation with the topographic surface and the stratigraphic boundary surfaces separating the stratigraphic units. In this model, the surfaces are represented in different colors: the topographic surface is represented in bluish colors, the Pre-Messinian top surface in yellowish, the Messinian in orangish-brownish, and the Post-Messinian in greyish colors (Fig. 7). Fig. 7 was constructed showing intermediate zenithal-lateral views with the boreholes and the four surfaces. With this kind of interpolation, the surfaces appear to be smooth and progressive. The figure shows different extension and changing height of surfaces. So, the Pre-Messinian top-surface shows deeper heights in the southern area and shallower up to exposed surface in the northern area. The Messinian top-surface is restricted to the southern half of the study area. The Post-Messinian top-surface (corresponding with the topographic surface) is represented in the whole area in the NW corner. Depocenters are inferred for the Post-Messinian stratigraphic unit. Nothing can be said about the depocenters during the deposition of the two lower stratigraphic units since they have been affected by erosion after their deposition and because of the depth of investigation was limited to 3.000 m b.s.l. In the case of the upper stratigraphic unit, depocenters are located in the right part of section B and C, and in the middle-right part of section E. This part belongs to the offshore area in front of the coast between Rocca di Neto and Cirò Marina. An uplifted area during the deposition of the upper stratigraphic unit can be located in the left part of section C and in the middle right part of section D. In this area the lower stratigraphic unit is

raised and the upper two ones are eroded or not deposited. This area belongs with the northern onshore area between Cirò and Nicola dell'Alto region.

4.5. Stratigraphic surfaces obtained with KNN interpolation

A new 3D HTML model, by using KNN interpolation, has been inferred with the topographic surface and the stratigraphic boundary surfaces separating the pre-and-post-Messinian stratigraphic units. In this model the surfaces are also represented with the different colors mentioned formerly. Fig. 8 was constructed showing intermediate zenithal-lateral and pure zenithal views with the boreholes and the four surfaces. With this kind of interpolation, the surfaces appear to be staggered and with abrupt steps. Equally to the former, the figure shows an overlap of the Post-Messinian top surface and erosion wedging of the Messinian top surface toward the N. Also, a rising of the Pre-Messinian top surface in the north area is here visible.

4.6. Recognized lineaments and structure

The 3D HTML model by using KNN interpolation represents all surfaces with stepped shape and net edges. These edges are lineaments in much cases corresponding with mapped faults from literature (Zecchin et al., 2012, 2013a, 2013b, 2020; Arcuri et al., 2023). Three main lineaments are testified with N–S, NNW-SSE and ENE-WSW oriented, that can be completed by a forth, E-W oriented (Fig. 8E to G). The result is a complex horts and grabens structure with a push up area in the northern onshore sector (between Cirò and Nicola dell'Alto) where the lower stratigraphic unit reaches the topographic one (Fig. 8B to D). Lineaments and horts-grabens structures are evident in the three represented surfaces.

4.7. Volumes of the stratigraphic units defined with Convex Hull application

Finally, the database also allowed to construct a new 3D HTML model by using Convex Hull (Fig. 9) with the volume estimation of the stratigraphic units. In this model the volumes are also represented in different colors: the Pre-Messinian unit in yellowish, the Messinian in
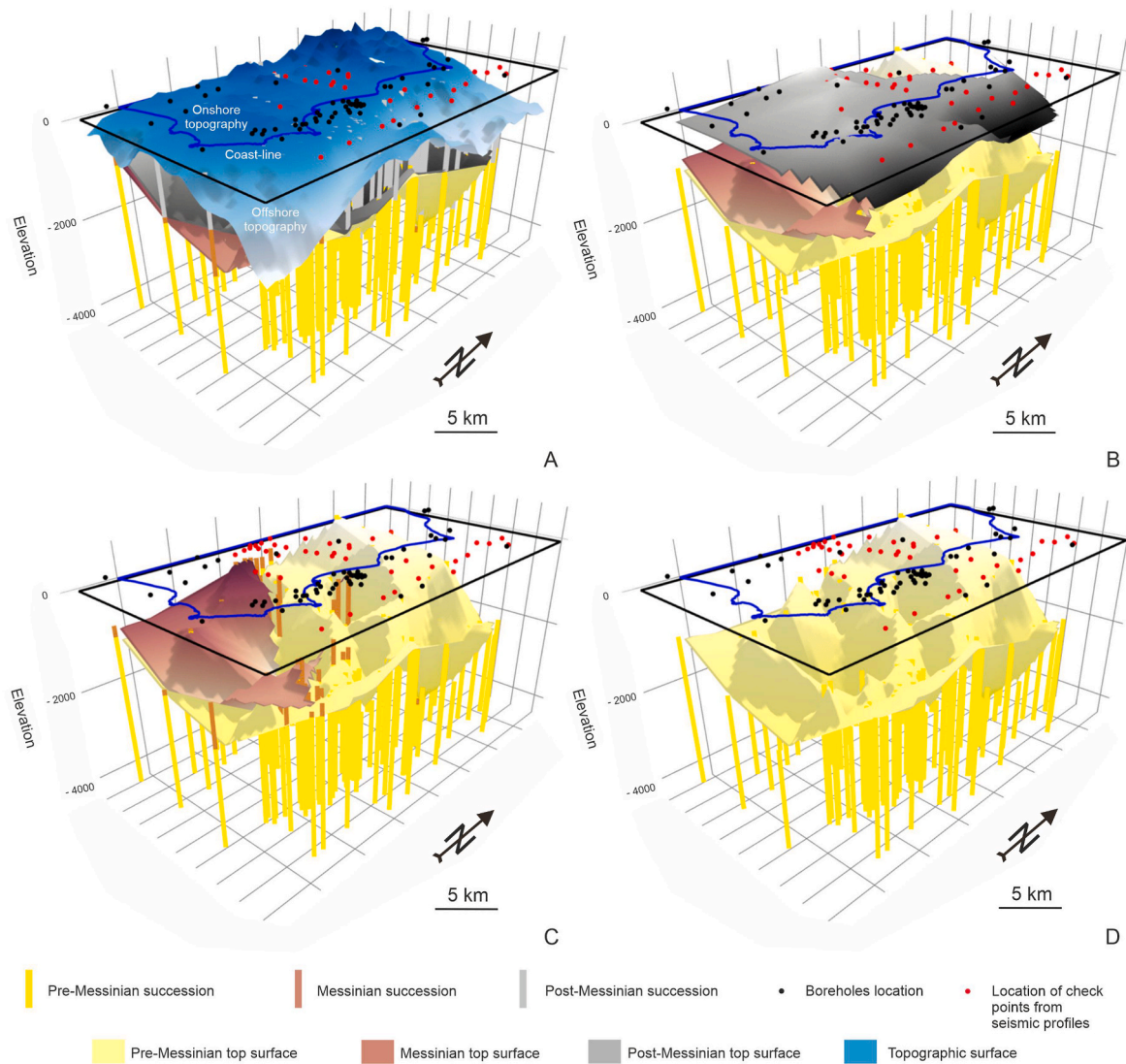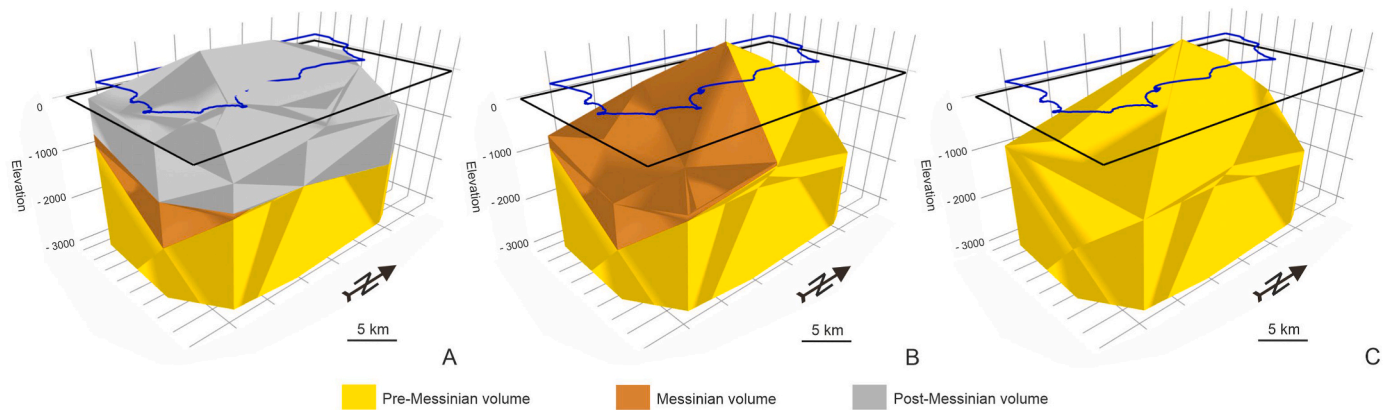
Fig. 7. Intermediate zenithal-lateral views of the 3D HTML model with the stratigraphic unit boundary surfaces obtained with linear interpolation: A) topographic and Pre-Messinian, Messinian and Post-Messinian top surfaces; B) Pre-Messinian, Messinian and Post-Messinian top surfaces; C) Pre-Messinian and Messinian top surfaces; D) Pre-Messinian top surface.
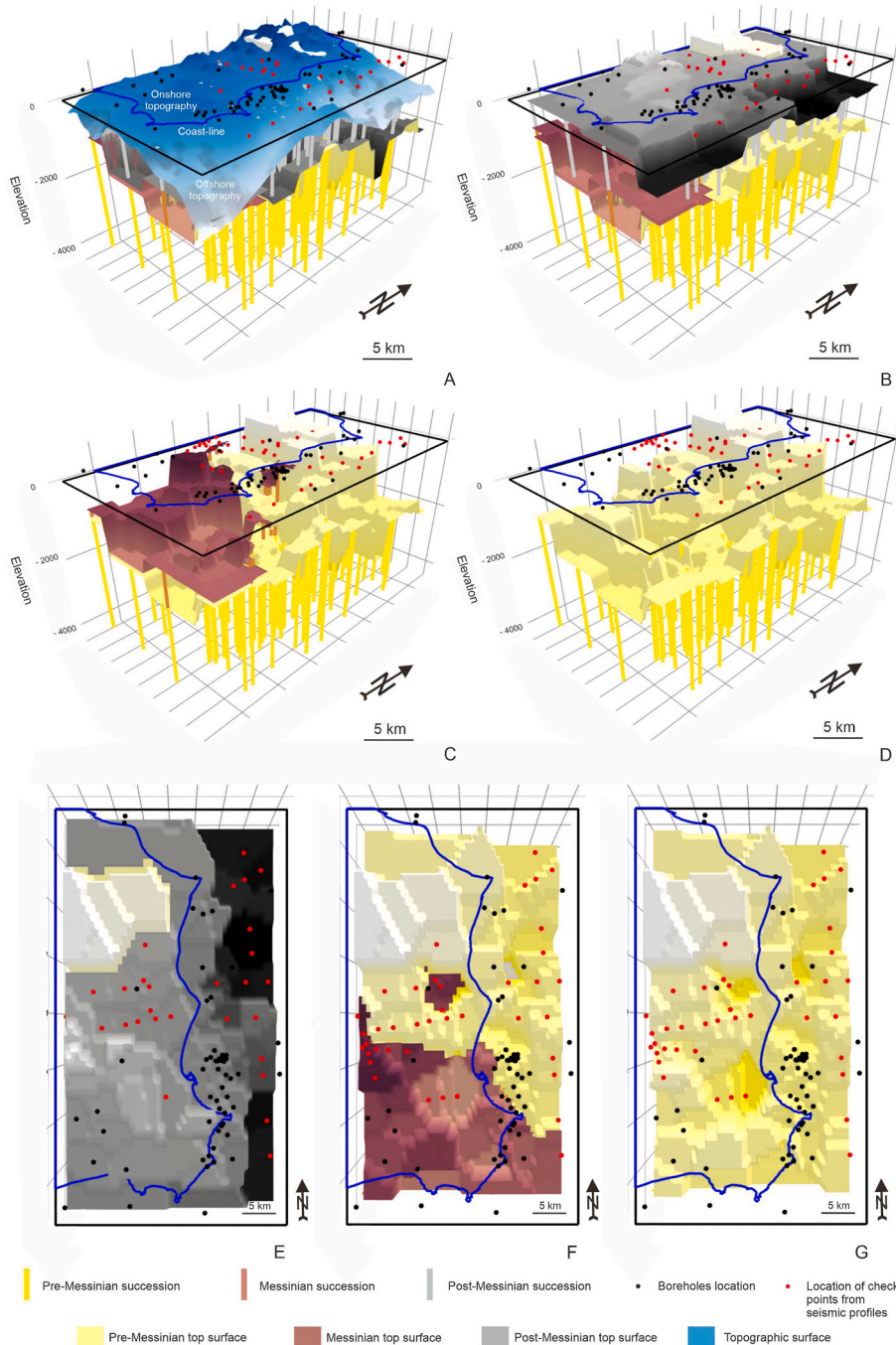
Fig. 8. Intermediate zenithal-lateral views (A to D) and zenithal views (E to G) of the 3D HTML model with the stratigraphic unit boundary surfaces obtained with KNN interpolation: A) topographic and Pre-Messinian, Messinian and Post-Messinian top surfaces; B) Pre-Messinian, Messinian and Post-Messinian top surfaces; C) Pre-Messinian and Messinian top surfaces; D) Pre-Messinian top surface; E Zenithal view with the Post-Messinian top surface and outcropping of the lower surfaces; F) Zenithal view with the Messinian top surface and outcropping of the Pre-Messinian top surface; G) Zenithal view with the Pre-Messinian top surface.

Fig. 9. Intermediate zenithal-lateral views of the 3D HTML model with the Convex Hull volumes: A) Pre-Messinian, Messinian and Post-Messinian volumes; B) Pre-Messinian and Messinian volumes; C) Pre-Messinian volume.

orangish-brownish, and the Post-Messinian in greyish colors. This model was also constructed following procedures by Bullejos et al. (2022a,b, 2023) and Martín-Martín et al. (2023a) where volumes can be automatically estimated with this methodology. According to the proposed model, Fig. 9 was constructed showing intermediate zenithal-lateral views of the volumetric balance. Fig. 9 testifies an overlap of the post-Messinian unit and an erosion wedging of the Messinian unit toward the N due to an abrupt rising of the pre-Messinian unit in that sector.

5. Discussion

5.1. Stratigraphic architecture and syn-tectonic sedimentation

An irregular extension and heights of the top-surfaces are registered in the study area (Fig. 7) related to the distribution of the three stratigraphic units. The defined surfaces are coincident with some of the unconformities from Zecchin et al. (2020). In detail, the pre-Messinian top surface corresponds with the second-order Tortonian unconformity, while the Messinian top surface is related to the first-order upper Messinian (Zecchin et al., 2020). Moreover, the defined stratigraphic units respectively correspond with the $CB1_1$-$CB1_2$ (Serravallian-Tortonian), $CB1_3$-$CB1_4$ (Messinian), and CB2-CB3 (Pliocene-Pleistocene) of Zecchin et al. (2020). This distribution provides further stratigraphic implications. Fig. 10 shows lateral views of the 3D HTML model with the stratigraphic unit boundary surfaces obtained with linear interpolation. In the case of boxes A to C (Fig. 10), the three top-surfaces are represented in southern lateral-view and correspond to sections A to Cfrom Fig. 6. In the case of boxes G to I (Fig. 10), the three top-surfaces are represented in eastern lateral-view and correspond to sections D and E from Fig. 6. In these boxes (Fig. 10), an overlap of the Post-Messinian top surface and an erosional truncation or not deposition of the Messinian stratigraphic unit toward the N is observed. Also, a rising of the Pre-Messinian stratigraphic unit in the northwestern area is appreciable. This onlapping stratigraphic architecture may indicate differentiate areas in subsidence and/or uplifting due to syn-sedimentary fault kinematics. To analyze the subsiding and rising areas, boxes D to F (based in sections A to Cof Fig. 6) and J-K (based in sections D and E of Fig. 6) have been constructed with the thickness by blocks in the vertical sections. In these boxes, subsiding and rising areas for each stratigraphic interval are reported. The Pre-Messinian uplifted area appears in the NW corner (boxes F and J in Fig. 10). The Messinian sedimentation is

restricted to the south half of the study area (boxes D and E, J and K in Fig. 10). The Messinian preferential subsiding areas are located in the central and eastern areas (boxes D and E, J and K in Fig. 10). The subsiding areas of the Post-Messinian interval appear in the central-north and eastern areas (boxes E, F and K in Fig. 10).

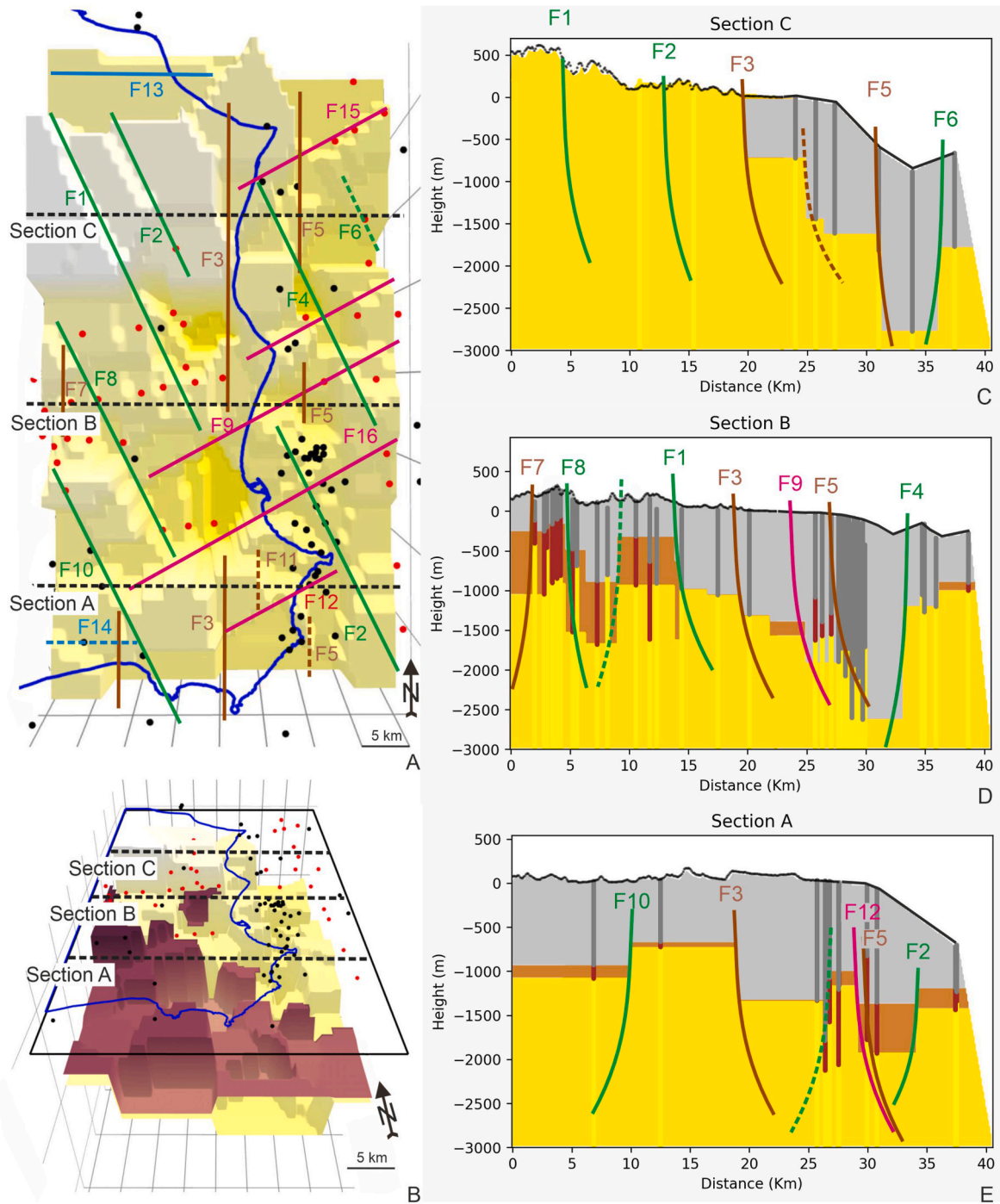### 5.2. Structural architecture and syn-sedimentary fault actuation

The 3D HTML model with the stratigraphic unit boundary surfaces obtained with KNN interpolation is in Fig. 8. By using this kind of interpolation, the surfaces appear with stepped and abrupt edges. Figs. 11 and 12 show the analysis in term of fault kinematics inferred from this 3D HTML. Both figures show a pure-zenithal view where the main set of faults are highlighted and labeled from F1 to F16 in box A. Oblique zenithal-lateral view are also represented in box B from both figures, with location of vertical cross-sections from Fig. 6 (southern view in the case of Fig. 11 and eastern view in the case of Fig. 12). Boxes C to D (Fig. 11), and C and D (Fig. 12) show reinterpreted sections A to E from Fig. 6 with location of the detected syn-sedimentary faults. These faults in the cross-sections are well correlated with the ones highlighted in boxes A of Figs. 11 and 12, and are also labeled and drawn in continuous line. Other intermediate faults not recognized in the boxes A of Figs. 11 and 12, are not labeled but they are drawn with dashed line in the cross-sections. Also, faults recognized in the sections and not in the 3D HTML are drawn with dashed lines in boxes A. Three main sets of faults can be inferred (Figs. 11 and 12): (1) the N–S fault set (drawn in brown color); (2) the NNW-SSE fault set (drown in green color): and (3) the ENE-WSW set (drawn in pink color). Also, a minor additional E-W fault set is also evident (drawn in blue color). These faults generated a horsts-grabens structure for the study area (boxes B from Figs. 11 and 12). In many cases a determinate set of faults generate a progressive descending or rising area with an "en echelon" major structure (boxes C to E from Fig. 11, and C and D from Fig. 12).

These sets of faults agree with the structural framework of the area (Van Dijk et al., 2000; Muto et al., 2014, 2017; Zecchin et al., 2020; Mangano et al., 2023a, 2023b) and most of these fault sets are interpreted as strike-slip fault ones (Fig. 13), making clear the benefits of this methodology by using Python.

The sedimentary infill of the basin, was allowed by the creation of accommodation space for deposition of the three stratigraphic units, through the effect of extensional Serravallian-Tortonian tectonic phase from Zecchin et al. (2020). The creation of the structure in horts-grabens
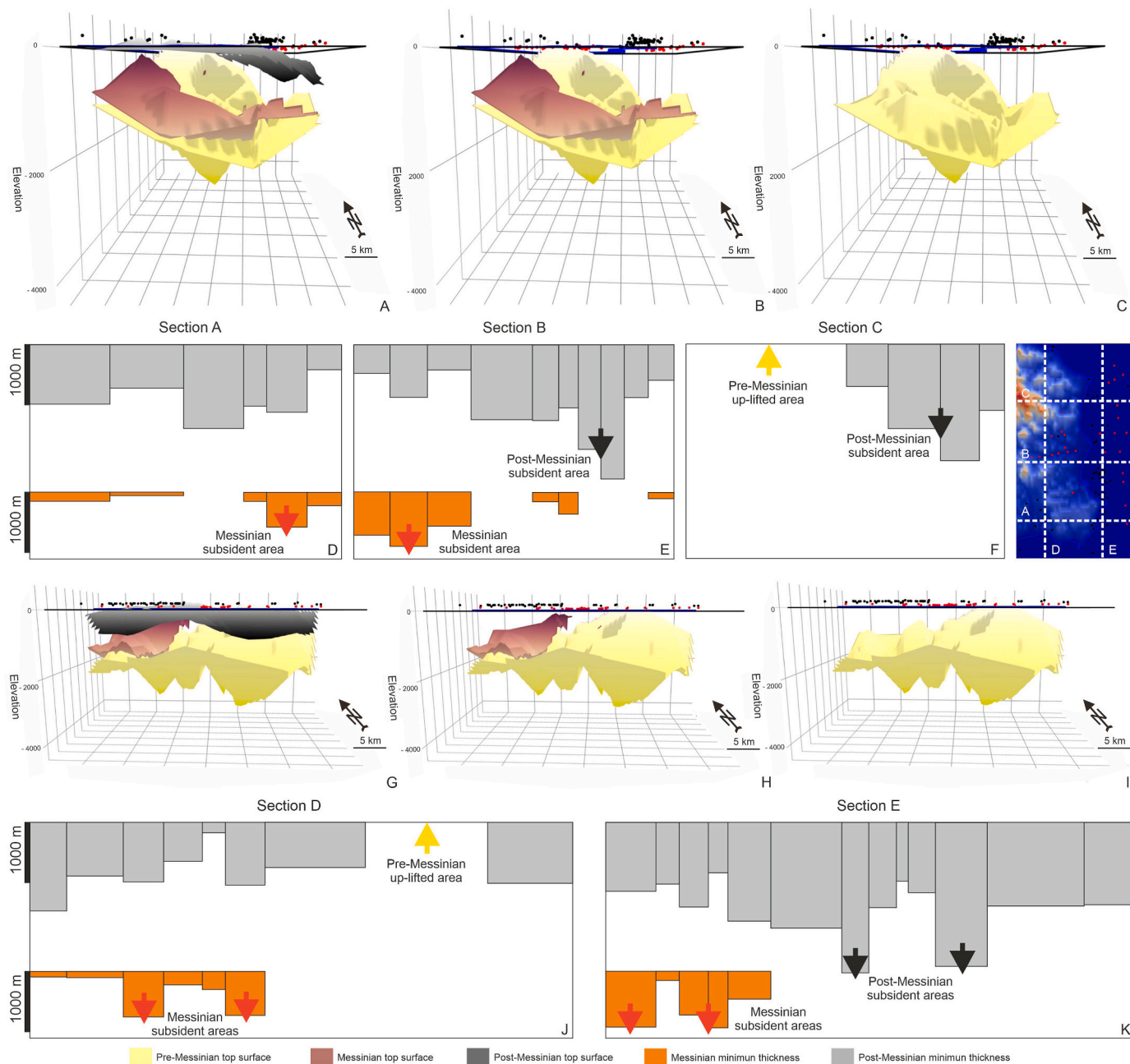
Fig. 10. Lateral views (A to C from the E; G to I from the S) of the 3D HTML model with the stratigraphic unit boundary surfaces obtained with linear interpolation, and thickness analysis of the Post-Messinian and Messinian stratigraphic units deduced from the vertical sections in Fig. 4: A) eastern view of the linear interpolation Pre-Messinian top, Messinian and Post-Messinian top surfaces; B) eastern view of the linear interpolation Pre-Messinian top and Messinian top surfaces; C) eastern view of the linear interpolation Pre-Messinian top surface; D) thicknesses analysis from section A; E) thicknesses analysis from section B; F) thicknesses analysis from section C; G) southern view of the linear interpolation Pre-Messinian top, Messinian and Post-Messinian top surfaces; H) southern view of the linear interpolation Pre-Messinian top and Messinian top surfaces; I) southern view of the linear interpolation Pre-Messinian top surface; J) thicknesses analysis from section D; K) thicknesses analysis from section E.

Fig. 11. Structural analysis with definition of possible faults derived from the 3D HTML model with the stratigraphic unit boundary surfaces obtained with KNN interpolation (Fig. 6) and the transversal vertical cross-sections (Fig. 4): A) pure zenithal view of the Pre-Messinian top surface with location of possible faults with labeling and location of sections A to C; B) oblique zenithal-lateral (from the S) view of the Pre-Messinian and Messinian top surfaces with location of sections A to C; C) Section A with location of possible faults and their labeling; D) Section B with location of possible faults and their labeling; E) Section C with location of possible faults and their labeling. Dashed lines indicate faults recognized only in vertical sections or in zenithal view of the 3D HTML model but not in the counter figure.
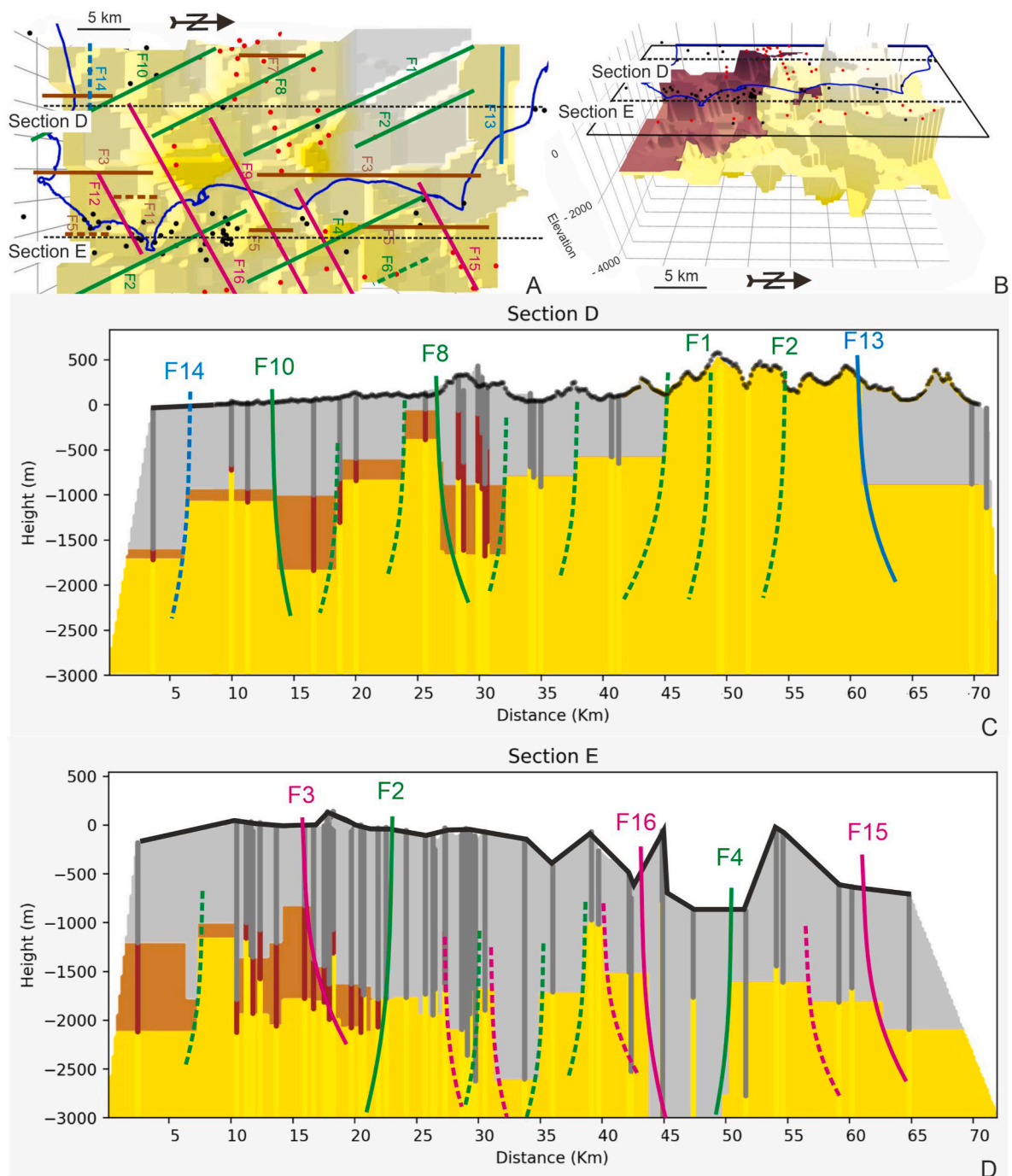
Fig. 12. Structural analysis with definition of possible faults derived from the 3D HTML model with the stratigraphic unit boundary surfaces obtained with KNN interpolation (Fig. 6) and the longitudinal vertical cross-sections (Fig. 4): A) pure zenithal view of the Pre-Messinian top surface with location of possible faults with labeling and location of sections D and E; B) oblique zenithal-lateral (from the E) view of the Pre-Messinian and Messinian top surfaces with location of sections D and E; C) Section D with location of possible faults and their labeling; D) Section E with location of possible faults and their labeling. Dashed lines indicate faults recognized only in vertical sections or in zenithal view of the 3D HTML model but not in the counter figure.

and the growing of the push-up structure between Cirò and Nicola dell'Alto area are inferred to be related to the Messinian tectonic phase by the same authors. Dome structures generated by halokinesis of the Messinian evaporites, inferred to be associated with normal faulting, were also documented in the Pliocene tectonic phase (Zecchin et al., 2003b). Finally, a contractional or transpressional Pleistocene phase is

related with the ultimate migration of northern Calabria toward the Apulian plate, as also proposed by Zecchin et al. (2020). Nevertheless, the model presented here shows that the main tectonic lineaments related with active faults and the structuring in horsts-grabens affect the three defined stratigraphic units (even to the post-Messinian one). This leads us to tentatively propose as main responsible of the present
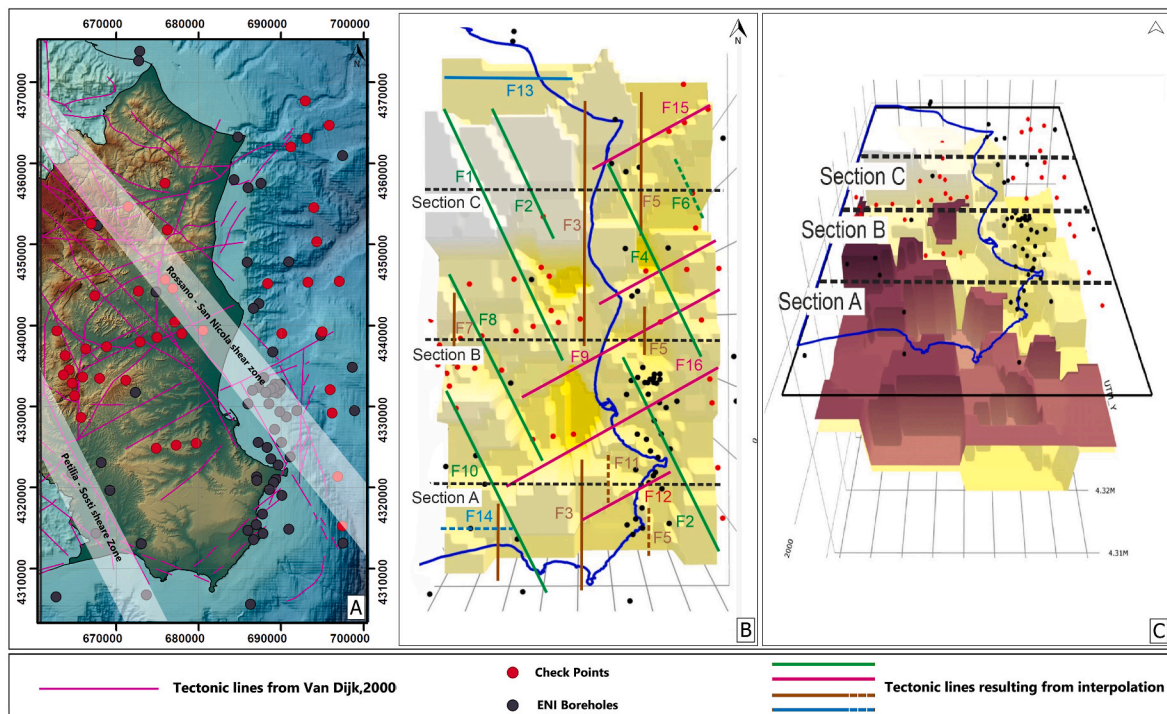
Fig. 13. Comparison of the structural framework of Crotone area (A) and the results obtained from the structural analysis by KNN interpolation (B and C).

structuring the post Messinian tectonic events (Pliocene and Pleistocene events), as highlighted also by Zecchin et al. (2020), giving less importance to the Messinian one.

6. Conclusion

- A dataset comprising 63 lithological records obtained from drilling exploration (16 onshore and 47 offshore boreholes) has been used. The areas with scarce or without information of direct boreholes, were implemented with 43 check points obtained from 9 interpreted seismic sections existing in the area.
- The data were grouped into three units (Pre-Messinian, Messinian and Post-Messinian stratigraphic units) and compiled into an XLS (Excel) file containing the boreholes locations and the check points position on seismic profiles, in the form of UTM coordinates and the elevation values of the top and bottom of the three defined units during the data homogenization phase.
- Different 3D HTML models were constructed using Python. Linear and KNN interpolation were implemented. Linear interpolation makes smoother the transition between points for stratigraphic interpretations, and a KNN interpolation resulting in sharper surfaces that give us clues to deduce the structural architecture of the basin. When KNN algorithm has been used, the parameters K = 1 was chosen.
- In a first step, the topographic and sea-level surface, the boreholes and the stratigraphic units from each borehole were obtained. Later, a serial 100 m-spaced of horizontal sections representing the three stratigraphic unit with different were implemented. Also, vertical sections were also created representing the study area with the boreholes and the check points from seismic profiles and exported to png files representing the three stratigraphic units. Finally, the database also allowed to construct a 3D HTML model by using Convex Hull with the volumes of the stratigraphic unit. With our procedures, volumes can be estimated.
- The above-mentioned 3D models also allowed deduce the stratigraphic architecture and syn-tectonic sedimentation for the study area. An overlap of the Post-Messinian top surface and an erosion

wedging of the Messinian top surface toward the N was observed. Also, a rising of the Pre-Messinian top surface in the northwestern area was visible.
- This onlapping stratigraphic architecture may indicate differentiate areas in subsidence and/or uplifting due to syn-sedimentary fault actuation. The Pre-Messinian uplifted area appeared in the NW corner while the Messinian sedimentation was restricted to the south half of the study area. The Messinian preferential subsiding areas are located in the central and eastern area, and the subsiding areas of the Post-Messinian interval appear in the central-north and eastern areas. This stratigraphic architecture agrees with the unconformities and depositional sequences mentioned in literature.
- The 3D HTML model with the stratigraphic unit boundary surfaces obtained with KNN interpolation (showing stepped and abrupt edges) allowed the interpretation in terms of structural architecture and syn-sedimentary fault actuation. Three main sets of faults were deduced: N–S; NNW-SSE, and ENE-WSW. To these main sets a minorly represented E-W set can be added.
- These faults generated a horsts-grabens structure for the study area. In many cases a determinate set of faults generates a progressive descended or rising area with an "en echelon" mayor structure. According to literature, these sets of faults have a good agreement with the structural cadre and defined faults of the area, making clear the benefits of this methodology using Python.

Websites

Albion: 3D geological models in QGIS.https://gitlab.com/Oslandia/albion.

GemPy: Open-source 3D geological modelinghttps://www.gempy.org.

GeoPandas. https://geopandas.org/en/stable.

GISgeography. 15 Python Libraries for GIS and Mapping. https://gisgeography.com/python-libraries-gis-mapping.

OSGeo: The Open Source Geospatial Foundation. https://www.osgeo.org/

Parpoil, B. Open source and geology. https://oslandia.com/en/2020

/07/09/geologie-open-source.

CRediT authorship contribution statement

Ettore Falsetta: Investigation, Formal analysis, Data curation. **Manuel Bullejos:** Formal analysis, Conceptualization. **Salvatore Critelli:** Funding acquisition, Data curation, Conceptualization. **Manuel Martín-Martín:** Methodology, Investigation, Funding acquisition, Formal analysis, Data curation, Conceptualization.

Declaration of competing interest

The authors declare that they have no known competing financial interests or personal relationships that could have appeared to influence the work reported in this paper.

Data availability

Data will be made available on request.

Acknowledgments

References

Adamczyk, J., Tiede, D., 2017. ZonalMetrics - a Python toolbox for zonal landscape structure analysis. Comput. Geosci. 99, 91–99. https://doi.org/10.1016/j.cageo.2016.11.005.

Arcuri, N., Muto, F., Chiarella, D., Critelli, S., 2023. The Miocene deposits of the Cirò Basin in the evolution of the peri-Ionian region, eastern Calabria. Rendiconti Online Soc. Geol. It. 59, 145–151. https://doi.org/10.3301/ROL.2023.24.

Barbera, G., Critelli, S., Mazzoleni, P., 2011. Petrology and geochemistry of Cretaceous sedimentary rocks of the Monte Soro Unit (Sicily, Italy): constraints on weathering, diagenesis and provenance. J. Geol. 119, 51–68. https://doi.org/10.1086/657340.

Barone, M., Dominici, R., Muto, F., Critelli, S., 2008. Detrital modes in a late Miocene wedge-top basin, northeastern Calabria, Italy: Compositional record of wedge-top partitioning. Journal of Sedimentary Research - J SEDIMENT RES. 78, 693–711. https://doi.org/10.2110/jsr.2008.071.

Bonardi, G., Cavazza, W., Perrone, V., Rossi, S., 2001. Calabria–peloritani terrane and northern ionian sea. In: Vai, G.B., Martini, I.P. (Eds.), Anatomy of an Orogen: the Apennines and Adjacent Mediterranean Basins. Kluwer Academic Publishers, Dordrecht, The Netherlands, pp. 287–306.

Borrelli, M., Perri, E., Critelli, S., Gindre-Chanu, L., 2021. The onset of the Messinian Salinity Crisis in the central Mediterranean recorded by pre-salt carbonate/evaporite deposition. Sedimentology 68, 1159–1197.

Borrelli, M., Perri, E., Avagliano, D., Coraggio, F., Critelli, S., 2022. Paleogeographic and sedimentary evolution of north Calabrian basins during the Messinian salinity crisis (south Italy). Mar. Petrol. Geol. 141, 105726 https://doi.org/10.1016/j.marpetgeo.2022.105726.

Brutto, F., Muto, F., Loreto, M.F., De Paola, N., Tripodi, V., Critelli, S., Facchin, L., 2016. The Neogene-quaternary geodynamic evolution of the central Calabrian arc: a case study from the western Catanzaro trough basin. J. Geodyn. 102, 95–114.

Bueno, A., Zuccarello, L., Díaz-Moreno, A., Woollam, J., Titos, M., Benítez, C., Álvarez, I., Prudencio, J., De Angelis, S., 2020. PICOSS: Python Interface for the classification of seismic Signals. Comput. Geosci. 142, 104531 https://doi.org/10.1016/j.cageo.2020.104531.

Bullejos, M., Cabezas, D., Martín Martín, M., Alcalá, F., 2022a. A Python application for visualizing the 3D stratigraphic architecture of the onshore Llobregat river Delta in NE Spain. Water 14. https://doi.org/10.3390/w14121882.

Bullejos, M., Cabezas, D., Martín Martín, M., Alcalá, F., 2022b. A K-nearest neighbors algorithm in Python for visualizing the 3D stratigraphic architecture of the Llobregat river Delta in NE Spain. J. Mar. Sci. Eng. 10, 986, 10.3390/2022.

Bullejos, M., Cabezas, D., Martín Martín, M., Alcalá, F., 2023. Confidence of a k-nearest neighbors Python algorithm for the 3D visualization of sedimentary porous media. J. Mar. Sci. Eng. 11, 60, 10.3390/2023.

Bullejos, M., Martín-Martín, M., 2023a. A Python application for visualizing an Imbricate thrust system: Palomeque Duplex (SE, Spain). Geosciences 13, 207. https://doi.org/10.3390/geosciences13070207.

Bullejos, M., Martín-Martín, M., 2023b. 3D Visualization of geological structures using Python: the case study of the Palomeque sheets (SE, Spain). J. Maps 19 (1), 2282593. https://doi.org/10.1080/17445647.2023.2282593.

Campilongo, G., Campilongo, E., Catanzariti, F., Muto, F., Ponte, M., Critelli, S., 2022. Subsidence analysis by mean of DeGloT software: application to the key-case of the Miocene-quaternary Crotone Basin (Calabria, S. Italy). Mar. Petrol. Geol. 146, 10596 https://doi.org/10.1016/j.marpetgeo.2022.105964.

Casanova-Arenillas, S., Rodríguez-Tovar, F.J., Martínez-Ruiz, F., 2020. Applied ichnology in sedimentary geology: Python scripts as a method toautomatize ichnofabric analysis in marine core images. Comput. Geosci. 136, 104407 https://doi.org/10.1016/j.cageo.2020.104407.

Cavalcanti Bezerra Guedes, V.J., Ramalho Maciel, S.T., Rocha, M.P., 2022. Refrapy: a Python program for seismic refraction data analysis. Comput. Geosci. 159, 105020 https://doi.org/10.1016/j.cageo.2021.105020.

Conforti, M., Muto, F., Rago, V., Critelli, S., 2014. Landslide inventory map of north-eastern Calabria (South Italy). J. Maps 10 (1), 90–102.

Corrado, S., Aldega, L., Perri, F., Critelli, S., Muto, F., Schito, A., Tripodi, V., 2019. Detecting syn-orogenic and sediment provenance of the Cilento wedge top basin (southern Apennines, Italy) by mineralogy and geochemistry of fine grained sediments and petrography of dispersed organic matter. Tectonophysics 750, 404–418. https://doi.org/10.1016/j.tecto.2018.10.027.

Costamagna, L., Criniti, S., 2024. Interpreting siliciclastic sedimentation in the upper Paleozoic Mulargia-Escalaplano basin (Sardinia, Italy): influence of tectonics on provenance. J. Palaeogeogr. 13 (1), 18–34. https://doi.org/10.1016/j.jop.2023.10.005.

Criniti, S., Borrelli, M., Falsetta, E., Civitelli, M., Pugliese, E., Arcuri, N., 2023a. Sandstone Petrology of the Crotone Basin, Calabria (Italy) from Well Cores, vol. 59. Rendiconti Online della Società Geologica Italiana. https://doi.org/10.3301/ROL.2023.10.

Criniti, S., Martín-Martín, M., Martín-Algarra, A., 2023b. New constraints for the western paleotethys paleogeography-paleotectonics derived from detrital signatures: Malaguide carboniferous culm cycle (Betic Cordillera, S Spain). Sediment. Geol. 458, 1–27. https://doi.org/10.1016/j.sedgeo.2023.106534, 106534.

Critelli, S., 1993. Sandstone detrital modes in the Paleogene Liguride complex, accretionary wedge of the southern Apennines (Italy). J. Sediment. Petrol. 63, 464–476. https://doi.org/10.1306/D4267B27-2B26-11D7-8648000102C1865D.

Critelli, S., 1999. The interplay of lithospheric flexure and thrust accomodation in forming stratigraphic sequences in the southern Apennines foreland basin system, Italy. Accademia Nazionale dei Lincei. Rendiconti Lincei. Sci. Fis. Nat. 10, 257–326. https://doi.org/10.1007/BF02904390.

Critelli, S., 2018. Provenance of Mesozoic to Cenozoic Circum-Mediterranean sandstones in relation to tectonic setting. Earth Sci. Rev. 185, 624–648. https://doi.org/10.1016/j.earscirev.2018.07.001.

Critelli, S., Muto, F., Tripodi, V., Perri, F., 2011. Relationships between lithospheric flexure, thrust tectonics and stratigraphic sequences in foreland setting: the Southern Apennines foreland basin system, Italy. In: Schattner, U. (Ed.), New Frontiers in Tectonic Research at the Midst of Plate Convergence. Intech Open Access Publisher, Janeza Trdine 9, Rijeka, Croatia, pp. 121–170. https://doi.org/10.5772/24120.

Critelli, S., Muto, F., Tripodi, V., Zecchin, M., Ceramicola, S., Ramella, R., Roda, C., 2014a. Note Illustrative Della Carta Geologica d'Italia Alla Scala 1:50.000, Foglio 554"Crucoli. ISPRA-Servizio Geologico d'Italia, p. 116 [Notes of the Geological Map of Italy at the scale 1: 50,000, Sheet 554 "Crucoli". ISPRA-Geological Survey of Italy, pp. 116].

Critelli, S., Muto, F., Zecchin, M., Tripodi, V., Ceramicola, S., Ramella, R., Roda, C., 2014b. Note Illustrative Della Carta Geologica d'Italia Alla Scala 1:50.000, Foglio 562"Cirò. ISPRA-Servizio Geologico d'Italia, p. 148 [Notes of the Geological Map of Italy at the scale 1:50,000, Sheet 562 "Cirò". ISPRA-Geological Survey of Italy, pp. 116].

Critelli, S., Muto, F., Perri, F., Tripodi, V., 2017. Interpreting provenance relations from sandstone detrital modes, southern Italy foreland region: stratigraphic record of the Miocene tectonic evolution. Mar. Petrol. Geol. 87, 47–59. https://doi.org/10.1016/j.marpetgeo.2017.01.026.

Critelli, S., Martín-Martín, M., 2022. Provenance, Paleogeographic and paleotectonic interpretations of Oligocene-Lower Miocene sandstones of the western-central Mediterranean region: a review, in the evolution of the Tethyan orogenic belt and, related mantle dynamics and ore deposits. Journal of Asian Earth Sciences Special Issue X8, 100124. https://doi.org/10.1016/j.jaesx.2022.100124.

Critelli, S., Martín-Martín, M., 2024. History of western Tethys Ocean and the birth of the circum-Mediterranean orogeny as reflected by source-to-sink relations. Int. Geol. Rev. 66 (2), 505–515. https://doi.org/10.1080/00206814.2023.2280787.

Di Grande, A., 1967. Sezione tipo della Molassa di San Mauro (Calabriano) nel bacino crotonese. Riv. It. Pal. Strat. 13, 199–271.

Fuentes, I., Padarian, J., Iwanaga, T., Willem Vervoort, R., 2020. 3D lithological mapping of borehole descriptions using word embeddings. Comput. Geosci. 141, 104516 https://doi.org/10.1016/j.cageo.2020.104516.

Gindre-Chanu, L., Borrelli, M., Caruso, A., Critelli, S., Perri, E., 2020. Carbonate/evaporitic sedimentation during the Messinian salinity crisis in active accretionary wedge basins of the northern Calabria, southern Italy. Mar. Petrol. Geol. 112, 104066.

Knott, S.D., Turco, E., 1991. Late cenozoic kinematics of the Calabrian arc, southern Italy. Tectonics 10, 1164–1172.

Krieger, L., Peacock, J.R., 2014. MTpy: a Python tool box for magnetotellurics. Comput. Geosci. 72, 167–175. https://doi.org/10.1016/j.cageo.2014.07.01.

Le Pera, E., Critelli, S., 1997. Sourceland controls on the composition of beach and fluvial sand of the Tyrrhenian Coast of Calabria, Italy: implications for actualistic petrofacies. Sediment. Geol. 110, 81–97. https://doi.org/10.1016/S0037-0738(96)00078-4.

Mangano, G., Zecchin, M., Civile, M., Ceramicola, S., Donato, A., Muto, F., Tripodi, V., Critelli, S., 2022. Mid-miocene to recent tectonic evolution of the Punta Stilo Swell (Calabrian arc, southern Italy): an effect of Calabrian arc migration. Mar. Geol. 448, 1–11. https://doi.org/10.1016/j.margeo.2022.106810, 106810.

Mangano, G., Alves, T.M., Zecchin, M., Civile, D., Critelli, S., 2023a. The Rossano-San Nicola fault zone evolution impacts the burial and maturation histories of the Crotone Basin, Calabrian arc, Italy. Petrol. Geosci. 29 (2), 1–22. https://doi.org/10.1144/petgeo2022-085.

Mangano, G., Ceramicola, S., Alves, T.M., Zecchin, M., Civile, D., Del Ben, A., Critelli, S., 2023b. A new large-scale gravitational complex discovered in the Squillace (central Mediterranean): tectonic implications. Sci. Rep. 1–12. https://doi.org/10.1038/s41598-023-40947-3 (2023) 13:14695.

Martín-Martín, M., Bullejos, M., Cabezas, D., Alcalá, F., 2023a. Using python libraries and k-Nearest neighbors algorithms to delineate syn-sedimentary faults in sedimentary porous media. Mar. Petrol. Geol. 153, 106283 https://doi.org/10.1016/j.marpetgeo.2023.106283.

Martín-Martín, M., Perri, F., Critelli, S., 2023b. Cenozoic detrital suites from the Internal Betic-Rif Cordilleras (S Spain and N Morocco): implications for paleogeography and paleotectonics. Earth Sci. Rev. 243, 1–16. https://doi.org/10.1016/j.earscirev.2023.104498, 104498.

Massari, F., Rio, D., Sgavetti, M., Prosser, G., D'Alessandro, A., Asioli, A., Capraro, L., Fornaciari, E., Tateo, F., 2002. Interplay between tectonics and glacio-eustasy: Pleistocene succession of the Crotone basin, Calabria (southern Italy). GSA Bull. 114, 1183–1209.

Massari, F., Prosser, G., Capraro, L., Fornaciari, E., Consolaro, C., 2010. A revision of the stratigraphy and geology of the south-western part of the Crotone Basin (South Italy). Ital. J. Geosci. (Boll. Soc. Geol. It.) 129 (3), 353–384.

Massari, F., Prosser, G., 2013. Late cenozoic tectono-stratigraphic sequences of the Crotone basin; insigths on the geodynamic history of the Calabrian Arc and Tyrrhenian sea. Basin Res. 25, 26–51.

Matot, L.S., Leung, K., Sim, J., 2011. Application of MATLAB and Python optimizer stotwocase studies involving groundwater flow and contaminant transport modeling. Comput. Geosci. 37, 1894–1899. https://doi.org/10.1016/j.cageo.2011.03.017.

Mattei, M., Cipollari, P., Cosentino, D., Argentieri, A., Rossetti, F., Speranza, F., Di Bella, L., 2002. The Miocene tectono-sedimentary evolution of the southern Tyrrhenian Sea: stratigraphy, structural and palaeomagnetic data from the on-shore Amantea basin (Calabrian Arc, Italy). Basin Res. 14, 147–168.

Mellere, D., Zecchin, M., Perale, C., 2005. Stratigraphy and sedimentology of faultcontrolled backstepping shorefaces, middle Pliocene of Crotone Basin, Southern Italy. Sediment. Geol. 176, 281–303.

Memari, S.S., Clement, T.P., 2021. PySWR- A Python code for fitting soil water retention functions. Comput. Geosci. 156, 104897. https://doi.org/10.1016/j.cageo.2021.10489.

Moretti, A., 1993. Note sull'evoluzione tettono-stratigrafica del bacino crotonese dopo la fine del Miocene. Boll. Soc. Geol. It. 112, 845–867.

Muto, F., Spina, V., Tripodi, V., Critelli, S., 2014. Tectonostratigraphic Neogene evolution of the allochthonous terrane in the eastern Calabrian foreland (southern Italy). Italian Journal of Geosciences 133, 455–473.

Muto, F., Tripodi, V., Chiarella, D., Lucà, F., Critelli, S., 2017. Tectono-stratigraphic architecture of the ionian piedmont between the Arso Stream and Nicà river catchments (Calabria, southern Italy). J. Maps 13, 332–341.

Ogniben, L., 1955. Le argille scagliose del Crotonese. Memorie e Note Istituto di Geologia Applicata di Napoli 6, 1–72.

Patacca, E., Sartori, R., Scandone, P., 1990. Tyrrhenian basin and Apenninic arcs: kinematic relations since Late Tortonian times. Memor. Soc. Geol. Ital. 45, 425–451.

Perri, E., Borrelli, M., Heimhofer, U., Umbro, B., Santagati, P., Le Pera, E., 2024. Microbial dominated Ca-carbonates in a giant Pliocene cold-seep system (Crotone Basin – south Italy). Sedimentology. https://doi.org/10.1111/sed.13192.

Perri, F., Critelli, S., Dominici, R., Muto, F., Tripodi, V., Ceramicola, S., 2012. Provenance and accommodation pathways of late quaternary sediments in the deep-water northern ionian basin, southern Italy, in Quantitative models in sediment generation. In: CRITELLI, S., von EYNATTEN, H., INGERSOLL, R.V., WELTJE, G. (Eds.), Sedimentary Geology Special Issue, vol. 280, pp. 244–259.

Roda, C., 1964. Distribuzione e facies dei sedimenti Neogenici nel Bacino Crotonese. Geol. Rom. 3, 319–366.

Rivillas-Ospina, G., Casas, D., Maza-Chamorro, M.A., Bolívar, M., Ruiz, G., Guerrero, R., Horrillo-Caraballo, H.M., Guerrero, M., Díaz, K., Del Rio, R., Campos, E., 2022. Appmar 1.0: a Python application for downloading and analyzing of WAVEWATCH III® wave and wind data. Comput. Geosci. 162, 105098 https://doi.org/10.1016/j.cageo.2022.105098.

Scharf, J., Chouchane, M., Finegan, D.P., et al., 2022. Bridging nano- and microscale X-ray tomography for battery research by leveraging artificial intelligence. Nat. Nanotechnol. 17, 446–459. https://doi.org/10.1038/s41565-022-01081-9.

Tonini, R., Sandri, L., Thompson, M.A., 2015. PyBetVH: a Python tool for probabilistic volcanic hazard assessment and for generation of Bayesian hazard curves and maps. Comput. Geosci. 79, 38–46. https://doi.org/10.1016/j.cageo.2015.02.017.

Tripodi, V., Muto, F., Critelli, S., 2013. Structural style and tectono-stratigraphic evolution of the Neogene-quaternary Siderno basin, southern Calabrian arc, Italy. Int. Geol. Rev. 55, 468–481.

Tripodi, V., Muto, F., Brutto, F., Perri, F., Critelli, S., 2018. Neogene-Quaternary evolution of the forearc and backarc regions between the Serre and Aspromonte Massifs, Calabria (southern Italy). Mar. Petrol. Geol. 95, 328–343. https://doi.org/10.1016/j.marpetgeo.2018.03.028.

Van Dijk, J.P., Okkes, F.W.M., 1990. The analysis of shear zones in Calabria; implications for the geodynamics of the Central Mediterranean. Riv. Ital. Strat. Paleont. 96, 241–270.

Van Dijk, J.P., 1990. Sequence stratigraphy, kinematics and dynamic geohistory of the Crotone Basin (Calabrian arc, central mediterranean): an integrated approach. Mem. Soc. Geol. Ital. 44, 259–285.

Van Dijk, J.P., 1991. Basin dynamics and sequence stratigraphy in the Calabrian Arc (central Mediterranean): records and pathways of the Crotone Basin. Geol. Mijnbouw 70, 187–201.

Van Dijk, J.P., Okkes, F.W.M., 1991. Neogene tectonostratigraphy and kinematics of Calabrian basins; implications for the geodynamics of the Central Mediterranean. Tectonophysics 196, 23–60.

Van Dijk, J.P., 1994. Late Neogene kinematics of intra-arc oblique shear zones: the petilia-Rizzuto fault zone (Calabrian Arc, central mediterranean). Tectonics 13, 1201–1230.

Van Dijk, J.P., Scheepers, P.J.J., 1995. Neogene rotations in the Calabrian arc. Implications for a Pliocene–recent geodynamic scenario for the central mediterranean. Earth Sci. Rev. 39, 207–246.

Van Dijk, J., Bello, M., Brancaleoni, G., Costa, V., Frixa, A., Golfetto, F., Merlini, S., Riva, M., Torricelli, S., Toscano, C., Zerilli, A., 2000. A regional structural model of the northern sector of the Calabrian Arc (Southern Italy). Tectonophysics 324, 267–320. https://doi.org/10.1016/S0040-1951(00)00139-6.

Zecchin, M., Massari, F., Mellere, D., Prosser, G., 2003b. Architectural styles of prograding wedges in a tectonically active setting, Crotone Basin, Southern Italy. Geological Society of London, Journal 160, 863–880.

Zecchin, M., Massari, F., Mellere, D., Prosser, G., 2004. Anatomy and evolution of a mediterranean-type fault bounded basin: the lower Pliocene of the northern Crotone Basin (southern Italy). Basin Res. 16, 117–143.

Zecchin, M., 2005. Relationships between fault-controlled subsidence and preservation of shallow-marine small-scale cycles: example from the lower Pliocene of the Crotone Basin (southern Italy). J. Sediment. Res. 75, 300–312.

Zecchin, M., Ceramicola, S., Gordini, E., Deponte, M., Critelli, S., 2011. Cliff overstep model and variability in the geometry of transgressive erosional surfaces in high-gradient shelves: the case of the Ionian Calabrian margin (southern Italy). Mar. Geol. 281, 43–58.

Zecchin, M., Caffau, M., Civile, D., Critelli, S., Di Stefano, A., Maniscalco, R., Muto, F., Sturiale, G., Roda, C., 2012. The Plio-Pleistocene evolution of the Crotone Basin (southern Italy): interplay between sedimentation, tectonics and eustasy in the frame of Calabrian Arc migration. Earth Sci. Rev. 115 (4), 273–303.

Zecchin, M., Civile, D., Caffau, M., Muto, F., Di Stefano, A., Maniscalco, R., Critelli, S., 2013a. The Messinian succession of the Crotone Basin (southern Italy) I: stratigraphic architecture reconstructed by seismic and well data. Mar. Petrol. Geol. 48, 455–473.

Zecchin, M., Caffau, M., Di Stefano, A., Maniscalco, R., Lenaz, D., Civile, D., Muto, F., Critelli, S., 2013b. The Messinian succession of the Crotone Basin (southern Italy) II: facies architecture and stratal surfaces across the Miocene-Pliocene boundary. Mar. Petrol. Geol. 48, 474–492.

Zecchin, M., Accaino, F., Ceramicola, S., Civile, D., Critelli, S., Da Lio, C., Mangano, G., Prosser, G., Teatini, P., Tosi, L., 2018. The Crotone megalandslide, southern Italy: architecture, timing and tectonic control. Scientific Reports Nature 8 (7778), 1–11. https://doi.org/10.1038/s41598-018-26266-y.

Zecchin, M., Civile, D., Caffau, M., Critelli, S., Muto, F., Mangano, G., Ceramicola, S., 2020. Sedimentary evolution of the Neogene-Quaternary Crotone Basin (Southern Italy) and relationships with large-scale tectonics: a sequence stratigraphic approach. Mar. Petrol. Geol. 117, 104381.

Zecchin, M., Mellere, D., Massari, F., Prosser, G., 2003a. Interplay between tectonics and sedimentation in the lower Pliocene fill of the Crotone Basin, Southern Italy, 12. AAPG/SEPM Annual Convention, Salt Lake City, Utah, p. 187.

Zecchin, M., Praeg, D., Ceramicola, S., Muto, F., 2015. Onshore to offshore correlation of regional unconformities in the Plio-Pleistocene sedimentary successions of the Calabrian Arc (central Mediterranean). Earth-Science Reviews 142, 60–78. https://doi.org/10.1016/j.earscirev.2015.01.006.